Archives of Gynecology and Obstetrics (2019) 300:1729–1739
https://doi.org/10.1007/s00404-019-05327-1

GYNECOLOGIC ENDOCRINOLOGY AND REPRODUCTIVE MEDICINE

Identification and characterization of uterine micro-peristalsis in women undergoing in vitro fertilization and embryo transfer via dynamic ultrasound features

Yunfei Long[1] · Rong Liang[2] · Jiabin Zhang[3] · Fang Fang[2] · Cheng Cheng[2] · Qun Lu[2] · Jue Zhang[1,3]

Received: 17 December 2018 / Accepted: 8 October 2019 / Published online: 23 October 2019

Abstract

Purpose This study aimed to identify the existence of uterine micro-peristalsis (UMP) by dynamic ultrasound features and evaluate the feasibility of UMP as a tool to distinguish pregnant and non-pregnant infertility patients undergoing in vitro fertilization–embryo transfer (IVF–ET), using clinical pregnancy results as a benchmark.

Methods Fifty-one women, including 29 pregnant and 22 non-pregnant patients were recruited. Also, ultrasound videos were collected before embryo transfer. First of all, undiscoverable uterine micro-peristalsis was magnified by video magnification. Then, the dynamic features of UMP were characterized by a novel index termed histogram entropy based on the micro-peristalsis feature selection by entropy weight (HEMEW), which was generated by combining frame difference and volume local phase quantization. Finally, a comparative experiment of HEMEW between non-pregnant and pregnant patients, logistic regression analysis for HEMEW and other independent clinical characteristics, and receiver operating characteristic (ROC) analysis were performed.

Results The magnified uterine video clearly exhibited UMP, which was invisible in the original ultrasound video. Further, there existed a significant difference in HEMEW between pregnant patients and non-pregnant patients after micro-motion magnification ($p=0.003$, $n=51$). The logistic regression result showed that HEMEW ($p=0.006$) was significantly associated with clinical pregnancy outcome, while other independent variables had no significant effect on it. The ROC performance of HEMEW was 72.6% accuracy (AUC = 0.774, 95% CI: 0.644–0.905).

Conclusions The proposed micro-motion magnification and characterization strategy identified the existences of uterine micro-peristalsis, and verified that UMP has the feasibility to distinguish the outcomes of IVF–ET.

Keywords Uterus · Infertility · In vitro fertilization and embryo transfer · Uterine peristalsis · Dynamic feature

Introduction

A global survey [1] conducted by the World Health Organization found that infertility affects one out of every seven couples on average, and in vitro fertilization and embryo transfer (IVF–ET) is a widely accepted treatment. IVF–ET's outcomes, however, may vary with different factors [2], including patient's age, basal serum follicle-stimulating hormone (bFSH) levels, infertility diagnosis, stimulation protocol, embryo quality, endometrium and so on. Among them, uterine receptivity and embryo quality are the two key determinants of IVF–ET's success [3–5], and some researchers even suggested that uterine receptivity accounts for about two-thirds [6] of IVF–ET failure. Accurate assessment of uterine receptivity is essential for IVF–ET success.

Electronic supplementary material The online version of this article (https://doi.org/10.1007/s00404-019-05327-1) contains supplementary material, which is available to authorized users.

✉ Qun Lu
luqun1023@sina.com

✉ Jue Zhang
zhangjue@pku.edu.cn

[1] College of Engineering, Peking University, NO. 5 Yiheyuan Road, Haidian District, Beijing 100871, People's Republic of China

[2] Center of Reproductive Medicine, Peking University People's Hospital, 100044, Beijing, People's Republic of China

[3] Academy for Advanced Interdisciplinary Studies, Peking University, NO. 5 Yiheyuan Road, Haidian District, Beijing 100871, People's Republic of China

Most previous studies on the factors affecting uterine receptivity focused on morphological features [7–9], such as endometrial thickness, endometrial type, and blood flow [10–12]. A few referred to dynamic indicators [13–15], and they only concerned one factor: visible uterine peristalsis. Actually, researchers [13] had noticed the importance of the uterine peristalsis in very early reproductive processes, like rapid and sustained directed sperm transport. Orisaka et al. [14] suggested that abnormal uterine peristalsis might be the cause of infertility associated with uterine leiomyoma. Zhu et al. [15] found that the uterine peristaltic wave frequency before embryo transfer was inversely related to the clinical pregnancy in fresh and frozen-thawed embryo transfer cycles. Above evidence indicated that uterine peristalsis in the endometrium might help to assess the uterine receptivity.

Unfortunately, the visible peristalsis wave is transient and inconvenient for the clinician to observe. Moreover, there is no uterine peristalsis in the uterus of some infertile women. Some experienced clinicians observe the uterus very carefully while the ultrasound probe stayed still, the uterus seems to have very micro-peristalsis in every place. However, the micro-peristalsis could not be observed in the regular clinical situation due to shaking probe and no awareness to observe it. These clinical experiences and difficulties inspire us to set up a hypothesis that there probably exist tiny peristalsis that can hardly be noticed by regular clinical procedures but may be strongly associated with clinical pregnancy outcomes of IVF–ET, and we name it as uterine micro-peristalsis (UMP).

Nevertheless, there is no available tool at present to observe UMP. Recently, phase-based video magnification [16] has revealed its unique power of invisible magnifying motion that existed in the video. In this study, inspired by the clinical experiences and the video magnification techniques, we will verify our hypothesis. Namely, there should exist UMP that can be revealed after video magnification.

Materials and methods

In our study, we recruited 51 women, including 22 non-pregnant patients and 29 pregnant patients of IVF–ET. First, UMP was made visible via video magnification. Second, a proposed index named histogram entropy based on the micro-peristalsis feature selection by entropy weight (HEMEW) was extracted to evaluate the UMP. Third, to reveal the contribution of video magnification [16] in distinguishing the outcome of IVF–ET patients, we compared the performance change before and after the magnification using HEMEW. Moreover, multivariate logistic regression analysis was used to assess the effect of HEMEW and other independent variables, including age, body mass index (BMI), stimulation protocol, number of embryos transferred, uterine position, endometrial thickness, and other factors. Finally, a receiver operating characteristic (ROC) analysis was made for HEMEW.

Study participants

This study was approved by the Ethics Committee of Peking University People's Hospital (approval number: 2018PHB150-01). Informed consent was provided by all participants. This study was conducted in a sample of 51 women who were undergoing IVF–ET and aged 32.7 ± 3.5 (mean $\pm$ standard deviation), with a BMI of 22.2 ± 3.1 kg. Twenty-nine of them had been confirmed to have clinical pregnancy, and the rest twenty-two had no clinical pregnancy. All patients had at least one available embryo to transfer, which eliminated the impact of embryo quality on results. The rate of miscarriage was 13.8%.

The inclusion criteria were as follows: (1) patients who were planning to undergo embryo transfer in 5 min; (2) 20 years $<$ age $\leq$ 40 years; (3) BMI was 17–32 kg/m^2; (4) basic FSH $<$ 12 IU/L. The exclusion criteria were as follows: (1) adenomyosis; (2) tubal hydronephrosis; (3) uterine fibroid; (4) intrauterine abnormality, e.g., endometrium polyp; (5) hyperprolactinemia; (6) thyroid disease; (7) chronic diseases which are not suitable for pregnancy; and (8) refusal to participate in the study. The recruiting process is shown in Fig. 1.

IVF–ET treatment protocols and clinical observation

The individual stimulation protocols for IVF–ET were determined according to the age of the patient and the ovarian reserve status, including the antral follicle count, basal levels of follicle-stimulating hormone (FSH), luteinizing hormone (LH), estradiol (E_2), and testosterone (T).Most women underwent the multi-dose gonadotropin-releasing hormone (GnRH) antagonist protocol (protocol I), which was initiated with a fixed dose of recombinant follicle-stimulating hormone (rFSH, 100–225 IU/day, 75 U/ampoule, GONAL-f®, Serono Ltd., Geneva, Switzerland) on cycle day 2 and co-treatment with a GnRH antagonist (Cetrotide®, 0.25 mg/day, Merck-Serono, Istanbul, Turkey) when the leading follicle was 13–14 mm in diameter. For the flare-up agonist stimulation (protocol II), a dose of rFSH along with a fixed dose of GnRHa (0.1 mg/day, triptorelin, Ferring, Saint-Prex, Switzerland), was administered beginning on menstrual day 2. For the long luteal down-regulation protocol (protocol III), 1.25 mg of gonadotropin-releasing hormone agonist (GnRHa, Diphereline®, Beaufour-Ipsen Pharmaceuticals Ltd., Paris, France) was injected on menstrual day 21. The initial gonadotropin dose was based on the physician's discretion, but always contained an amount of rFSH, supplemented with at least one ampoule (75 IU) of human menopausal gonadotropin (HMG). Human chorionic

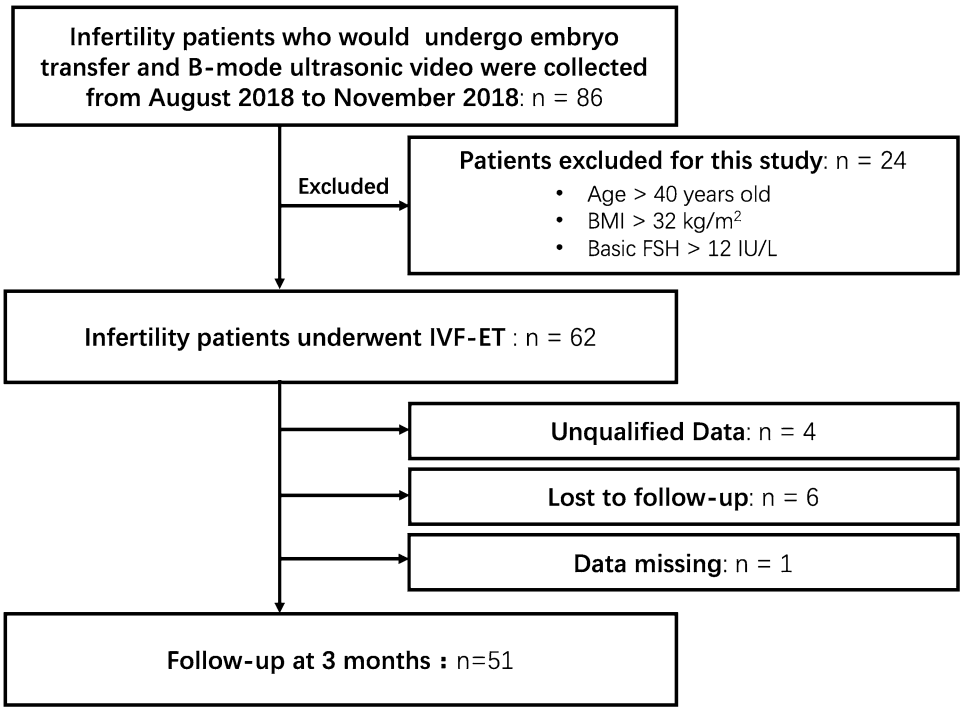

Fig. 1 The recruitment flow chart with exclusion criteria

gonadotropin (HCG, 10,000 IU, Lizhu Ltd., Guangdong, China) was administered when at least two follicles achieved 18 mm in diameter. Oocytes were retrieved by transvaginal ultrasound-guided follicular aspiration 36 h later. Oocytes were fertilized using either standard IVF insemination or intracytoplasmic sperm injection (ICSI) depending on the semen quality of the partner and IVF history. For couples with male factor, such as severe oligozoospermia (the sperm concentration less than 5 million per milliliter), asthenospermia (caveat for 90% immotile spermatozoa), teratozoospermia (less than 1% normal morphology by strict criteria including globozoospermia), ejaculatory disorders (e.g., electro-ejaculation, retrograde ejaculation), azoospermia, and couples with repeated total fertilization failure and low fertilization (fertilization rate < 25%) after conventional IVF, ICSI was performed. Half ICSI was half the number of oocytes fertilized by IVF and the sibling oocytes fertilized by ICSI, which was performed when sperm parameters were borderline.

The fertilization results (two pronuclei, 2PN) were assessed 16–20 h after insemination. High-quality embryos were defined as embryos developed from normally fertilized eggs, with no fragmentation or no more than 10% fragmentation, no presence of multinucleation, and 7–8 blastomeres 72 h after egg retrieval. One or two embryos per patient were transferred under ultrasonic guidance on the 3rd or 5th day after oocyte retrieval. The fresh embryos were transferred when the progesterone (P) level on the HCG delivery day was below 1.5 ng/mL with normal endometrium thickness and no risk of ovarian hyperstimulation syndrome. Otherwise, the embryos were frozen, and frozen embryo transfer was performed after 2 months. The endometrium was prepared for frozen embryos transfer using two protocols. For the women with ovulation, ultrasound monitoring evaluation of the dominant follicle occurred from days 9 to 11 and continued until the dominant follicle reached 16–20 mm in diameter. Oral dydrogesterone (Duphaston, Abbott, OLST, Netherlands) 20 mg twice daily was administered for luteal phase support after ovulation. One or two day-3 or day-5 frozen embryos were transferred on day 3 or day 5 after ovulation. For women with anovulation, oral estrogen (progynovaw 6 mg, daily; Bayer, Leverkusen, Germany) were administered from day 2 or day 3. When the endometrial thickness reached ≥ 8 mm, vaginal micronized progesterone (Crinone®, Merck Serono, Switzerland) 90 mg daily and oral dydrogestrone 20 mg daily or intramuscular progesterone 80 mg (20 mg/ampoule, Xianju Ltd., Zhejiang, China) was administered. On day 4 of the progesterone regimen, one or two day-3 frozen embryos were thawed and transferred. Day-5 frozen embryos were transferred after 6 days of progesterone preparation.

A positive pregnancy was defined as a β-hCG level > 25 IU/L on the 14th day after embryo transfer. Clinical pregnancy was confirmed by positive fetal cardiac activity and the number of sacs using a vaginal ultrasound after a 6-week gestation. If the clinical pregnancy was achieved, luteal phase support was continued until 10-week gestation. Ongoing pregnancy was defined as the presence of a fetus with heart motion at 11–12 weeks of gestation. Demographic characteristics, controlled ovarian

Table 1 Demographic characteristics and controlled ovarian hyperstimulation parameters of patients who underwent IVF–ET

Characteristics	Total ($n=51$)	Pregnancy ($n^a=29$)	Non-pregnancy ($n=22$)	p^c
Age (year)	32.75 ± 3.52	33.21 ± 3.30[b]	32.14 ± 3.80	0.121
BMI (Kg/m^2)	22.25 ± 3.09	22.89 ± 3.44	21.41 ± 2.41	0.074
Fasting glucose (nmol/L)	5.17 ± 0.44	5.21 ± 0.50	5.12 ± 0.34	0.012
Fasting insulin (uU/ml)	10.31 ± 6.42	11.27 ± 7.98	9.04 ± 3.23	0.094
Insulin resistance	3.07 ± 4.13	2.65 ± 2.02	3.63 ± 5.89	0.939
Indication of IVF				
Primary infertility	31 (60.8%)	15 (48.4%)	16 (51.6%)	0.128
Secondary infertility	20 (39.2%)	14 (70.0%)	6 (30.0%)	
Tubal factor	26 (60.0%)	13 (50.0%)	13 (50.0%)	0.318
Male	35 (68.6%)	21 (60.0%)	14 (40.0%)	0.503
Polycystic ovary syndrome (PCOS)	4 (7.8%)	3 (75.0%)	1 (25.0%)	0.445
Endometriosis	12 (23.5%)	7 (58.3%)	5 (41.7%)	0.906
Poor ovarian response (POR)	5 (9.8%)	2 (40.0%)	3 (60.0%)	0.423
Antral follicle count (n)	10.47 ± 6.51	10.81 ± 4.82[b]	10.05 ± 8.23	0.061
Basal FSH levels (IU/L)	8.59 ± 5.38	8.32 ± 4.88	8.89 ± 5.99	0.419
Basal LH levels (IU/L)	4.39 ± 2.82	4.47 ± 2.04	4.30 ± 3.59	0.149
Basal E2 levels (nmol/L)	40.93 ± 24.38	33.99 ± 19.62	45.42 ± 22.93	0.773
Basal T levels (nmol/L)	2.52 ± 2.34	2.66 ± 2.56	2.32 ± 2.21	0.657
Stimulation protocol				
Protocol I	40 (78.4%)	21 (52.5%)	19 (47.5%)	0.412
Protocol II	1 (2.0%)	1 (100%)	0 (0.0%)	
Protocol III	10 (19.6%)	7 (70.0%)	3 (30.0%)	
Days of stimulation	9.82 ± 2.93	9.59 ± 1.92	10.14 ± 3.92	0.274
Starting dose of gonadotropins (IU)	2.33 ± 0.65	2.45 ± 0.686	2.18 ± 0.588	0.057
Total dose of gonadotropins (IU)	28.28 ± 9.67	27.86 ± 7.07	28.84 ± 12.468	0.145
Number of follicles > 13 mm	9.06 ± 5.04	9.52 ± 4.74	8.45 ± 5.46	0.556
LH levels on the HCG day (IU/L)	4.63 ± 4.40	3.77 ± 3.68	5.73 ± 5.07	0.041
E2 levels on HCG day (nmol/L)	2386.44 ± 1484.19	2470.18 ± 1501.47	2282.77 ± 1492.68	0.791
P levels on HCG day (nmol/L)	1.35 ± 0.72	1.34 ± 0.79	1.37 ± 0.65	0.218
Insemination method				
IVF	24 (47.1%)	16 (66.7%)	8 (33.3%)	0.119
ICSI	19 (37.3%)	11 (57.9%)	8 (42.1%)	
Half ICSI	8 (15.7%)	2 (25.0%)	6 (75.0%)	
Number of oocytes retrieved	10.44 ± 6.63	11.18 ± 6.48	9.50 ± 6.84	0.765
Number of MII oocytes	8.56 ± 5.54	9.11 ± 5.82	7.86 ± 5.20	0.967
Number of 2PN	6.34 ± 4.07	6.86 ± 4.24	5.68 ± 3.83	0.944
Number of high-quality embryos	1.96 ± 1.64	2.14 ± 1.67	1.73 ± 1.61	0.634
Cycles of transferred embryo				
Fresh	9 (17.6%)	5 (55.6%)	4 (44.4%)	0.930
Frozen	42 (82.4%)	24 (57.1%)	18 (42.9%)	
Day of embryo transfer				
Day 3	32 (62.7%)	20 (62.5%)	12 (37.5%)	0.291
Day 5	19 (37.3%)	9 (47.4%)	10 (52.6%)	
Number of transfer embryo				
1	8 (15.7%)	5 (62.5%)	3 (37.5%)	0.726
2	43 (84.3%)	24 (55.8%)	19 (44.2%)	
Endometrial thickness on transplanted day (cm)	0.93 ± 0.17	0.94 ± 0.19	0.92 ± 0.16	0.686
Uterine position				
Anteflexion	34 (66.7%)	21 (61.8%)	13 (38.2%)	0.422
Horizontal	4 (7.8%)	1 (25.0%)	3 (75.0%)	
Retroversion	13 (25.5%)	7 (53.9%)	6 (46.1%)	

[a]Number of subjects

[b]Data were shown as mean value ± standard deviation

Table 1 (continued)

[c]Mann–Whitney *U* test

hyperstimulation parameters, and pregnancy outcomes were obtained through review of medical records, which are shown in Table 1.

Standardized protocol of data collection

Probe orientation and video quality are highly operator dependent [17]. To overcome this difficulty, we have set up a standardized scanning protocol to reduce the influence of the operator. In this study, only one operator (clinician) did the scan according to the following protocol:

1. disinfect the probe fixer by spraying with alcohol;
2. let the patient lie flat, keep the body still and breath normally;
3. find the section of the uterus with the largest longitudinal section and fix the transvaginal probe with the probe fixer;
4. collect video data for 2 min;
5. remove the transvaginal ultrasound (TVUS) probe from the patient's vagina after data collection.

Video processing and modeling

Figure 2 illustrates the procedure of extracting HEMEW index from patients, which includes five steps: video collection, the uterine region of interest (ROI) extraction, UMP magnification, frames difference, and dynamic feature extraction.

Video collection A 10-s transvaginal ultrasonic B-mode video was collected from each patient through the ultrasound equipment. The ultrasound equipment was an ultrasound device (ALOKA F37, Hitachi, Ltd., Tokyo, Japan) and the ultrasound probe was a transvaginal ultrasound probe with a scanning frequency of 6–9 MHz and scanning angle ranging between 85° and 120°. Each patient was required to remain physically still and was scanned by a transvaginal ultrasound probe. Instead of asking the operator to keep the probe physically still, we designed a probe fixer to do the job and obtained stable images. The sampling rate of the ultrasound video is 30 Hz.

Uterine ROI extraction The uterine ROI was easily selected by a general physician. The ROI is a rectangular box

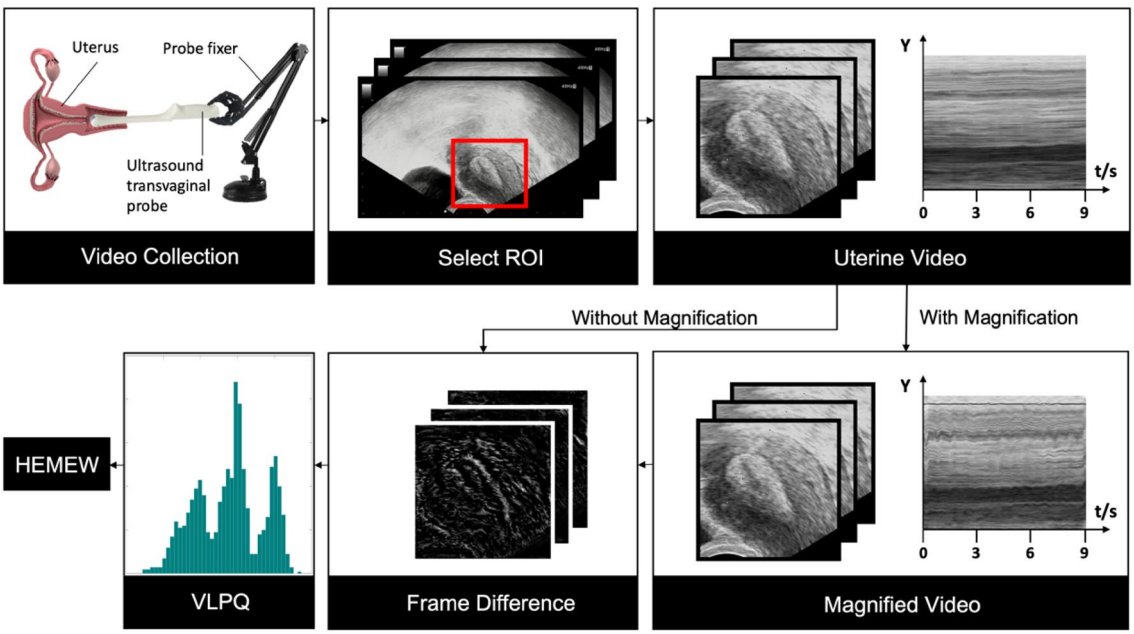

Fig. 2 Procedure of the proposed method. Initially, the original video was collected by ultrasound transvaginal probe with a probe fixer. Second, uterus ROI was selected from the original video by a general physician. Then, phase-based video magnification was applied to magnify the uterine micro-peristalsis. Two adjacent frame difference method was applied both for the uterine video and the corresponding magnified video. Afterward, volume local phase quantization (VLPQ) was utilized to extract the spatial–temporal features of uterine micro-peristalsis. Finally, the index HEMEW was extracted

containing uterus in the video. And then we normalized the uterine videos into a resolution of 256 × 256.

UMP magnification Thus we deployed the phase-based video magnification [16] technique to magnify the UMP in the video. The parameters of phase-based video magnification were set as: magnification factor = 10, the magnification frequency range = 1–1.7 Hz, the weighted filter coefficient = 5, and frame rate = 30 Hz.

Frames difference Frame difference method was applied to both the uterine video and magnified video, respectively.

Dynamic feature extraction Volume local phase quantization (VLPQ) is a descriptor for dynamic texture analysis, which is a spatiotemporal version of local phase quantization [18]. After phase-based video magnification, the VLPQ algorithm was then applied to extract the dynamic features of uterine micro-peristalsis. The parameters of the VLPQ algorithm were set as: window size = 27, planes = 19, eigenvalues = 10; the correlation coefficients used in the case of VLPQ were $\rho_s = 0.1$, and $\rho_t = 0.1$; and normalization was adopted in all 1024 features of output.

The distribution of dynamic characteristics was depicted by a new index, termed histogram entropy based on the micro-peristalsis features selection of entropy weight (HEMEW). HEMEW was created to depict uterine micro-peristalsis. The method to obtain HEMEW is as follows:

(a) calculate the entropy weight [19] of DCD. DCD (dynamic characteristics distribution) stood for the 1024 features extracted by the vLPQ algorithm. The method for calculating entropy weight w_j could be divided into four parts. First, the DCD should be normalized (Eq. 1), where m is the number of subjects, x_{ij} is the features of DCD; then, computing the entropy of each feature, where n is the number of features from DCD (Eqs. 2, 3); third, entropy weight was calculated (Eq. 4).

$$r_{ij} = \frac{x_{ij}}{\sum_{i=1}^{m} x_{ij}}, \quad i = 1, 2, \ldots, m \tag{1}$$

$$e_j = -s \sum_{i=1}^{m} r_{ij} \ln r_{ij}, \quad j = 1, 2, \ldots, n \tag{2}$$

$$s = \frac{1}{\ln(m)} \tag{3}$$

$$w_j = \frac{1 - e_j}{\sum_{j=1}^{n} (1 - e_j)}, \quad j = 1, 2, \ldots, n \tag{4}$$

(b) select the top k ($k = 1, 2, 4, \ldots, 1024$) features based on the entropy weight . As there were somany useless features according to entropy weight analysis, we chose $k = 108$;
(c) obtain the histogram of (b) result h_q. Bin of the histogram was a hyper-parameter, which was chosen as 75;
(d) calculate the entropy of histogram from (c), and the entropy was HEMEW. $f(h_q)$ is the probability distribution of h_q, $Q = 100$, $R = 3$.

$$HEMEW = Q * \left(R - \sum_{q=1}^{k} f(h_q) \log h_q \right), \quad q = 1, 2, \ldots, k \tag{5}$$

Statistical analysis

First, we applied the Mann–Whitney U test to demographic characteristics one by one, such as age, BMI, fasting glucose, and fasting insulin. Second, the Wilcoxon rank-sum test was applied to HEMEW, which was generated from the videos before and after the magnification to reveal the contribution of the UMP's magnification further. Then, multivariate binary logistic regression analysis model was utilized to assess the effect of HEMEW and other independent factors. The dependent variable was the outcome of clinical pregnancy. The independent variables were shown in Table 2. At last, to find the optimal cutoff values for HEMEW, ROC analysis was performed, and the area under the curve (AUC) was determined. ROC curves were produced by plotting sensitivity against 1-specificity. The optimal cutoff value for ROC curves was established using the Youden Index (YI = sensitivity + specificity − 1). In the ROC analysis, if the HEMEW of IVF patients was higher than the cutoff value, its predict result would be pregnant; on the contrary, if the HEMEW of IVF patients was lower than the cutoff value, its predicted result would be not pregnant. All the statistical analyses were facilitated by software SPSS statistics (version 25, IBM, USA), and we set p value less than 0.05 to indicate statistical significance ($^*p < 0.05$; $^{**}p < 0.01$; $^{***}p < 0.001$).

Results

Qualitative results

The UMP is the micro-peristalsis that occurs in various directions and frequencies in the endometrium and myometrium. We plotted spatiotemporal evolutions of UMP in YT (Y axis and time axis) slice (Figs. 3, 4). The YT slice is the same as M-mode ultrasound. As demonstrated in Figs. 3 and 4, typical uterine micro-peristalsis, namely UMP, can be more easily observed after video magnification. Typical

Table 2 Multiple logistical regression analyses of possible determinants for clinical pregnancy

Factor	OR[a] (95% CI)	*p* value
HEMEW	1.492 (1.120–1.989)	0.006
Age	1.204 (0.926–1.564)	0.166
BMI	1.398 (0.902–2.168)	0.134
Insulin resistance	0.817 (0.541–1.233)	0.336
Number of transfer embryo	0.465 (0.023–9.472)	0.619
Endometrial thickness on transplanted day	0.198 (0.001–43.867)	0.556
Day of embryo transfer	0.899 (0.088–9.133)	0.928
Uterine position		
Anteflexion	–	0.636
Horizontal	0.714 (0.090–5.679)	0.750
Retroversion	0.219 (0.010–5.016)	0.342
Antral follicle count		0.959
bFSH		0.850
Stimulation protocol		
Protocol I[c]	2.923 (0.282–30.247)	0.667
Protocol II[d]	NA[b]	0.368
Protocol III[e]	–	1.000

[a]The OR was calculated from the multiple logistic regression analyses after controlling for other variables

[b]NA is short for not available. There was only one pregnant patient stimulated by Protocol II, which could not compute OR value

[c]The multi-dose GnRH antagonist protocol

[d]The flare-up agonist stimulation

[e]The long luteal down-regulation protocol

videos (Video 1, Video 2) of a non-pregnant patient and a pregnant patient with and without magnification are available in supplementary materials. Practically, clinicians could still hardly predict the outcomes of IVF–ET through motion-magnified videos due to the inenarrable peristaltic pattern of UMP. Thus, a way to define UMP characteristics and patterns has become essential.

Quantitative results

Qualitative results encouraged us to describe UMP as a novel index through pattern recognition. Therefore, we adopted VLPQ to extract the spatial–temporal features of the UMP after frame difference. And the results, namely typical DCD of a non-pregnant and a pregnant patient, are exhibited in Fig. 5.

The results of the Wilcoxon rank-sum test (Fig. 6) show that there was a remarkable difference in HEMEW between non-pregnant patients and pregnant patients after video magnification ($p < 0.01$, $n = 51$). Further, there was a significant difference in HEMEW between non-pregnant patients with magnification and without magnification ($p < 0.001$, $n = 51$). The HEMEW was also significant between pregnant patients with magnification and without magnification ($p < 0.01$, $n = 51$). By comparison, there was no significant difference in HEMEW between non-pregnant patients and pregnant patients without magnification ($p > 0.05$, $n = 51$). These results indicated that the video magnification could magnify the UMP by increasing the signal-to-noise ratio of UMP. That is to say, the video magnification can magnify the signal of UMP.

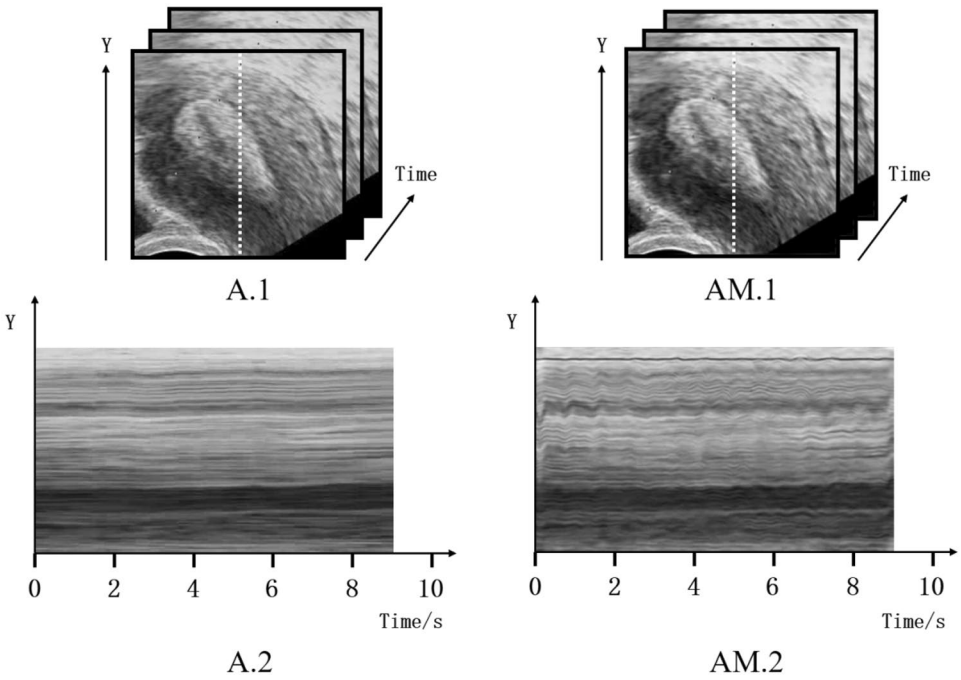

Fig. 3 Comparison of uterus video and magnified video from a typical non-pregnant patient (**A**) of IVF–ET. **A.1** represents the uterus video; **AM.1** represents the corresponding magnified video. **A.2** is the spatiotemporal YT slice of the uterine video, which is generated by the white dotted line's *Y* axis in uterus video. **AM.2** is the spatiotemporal YT slice of magnified video, which is generated by the white dotted line's *Y* axis in the magnified video

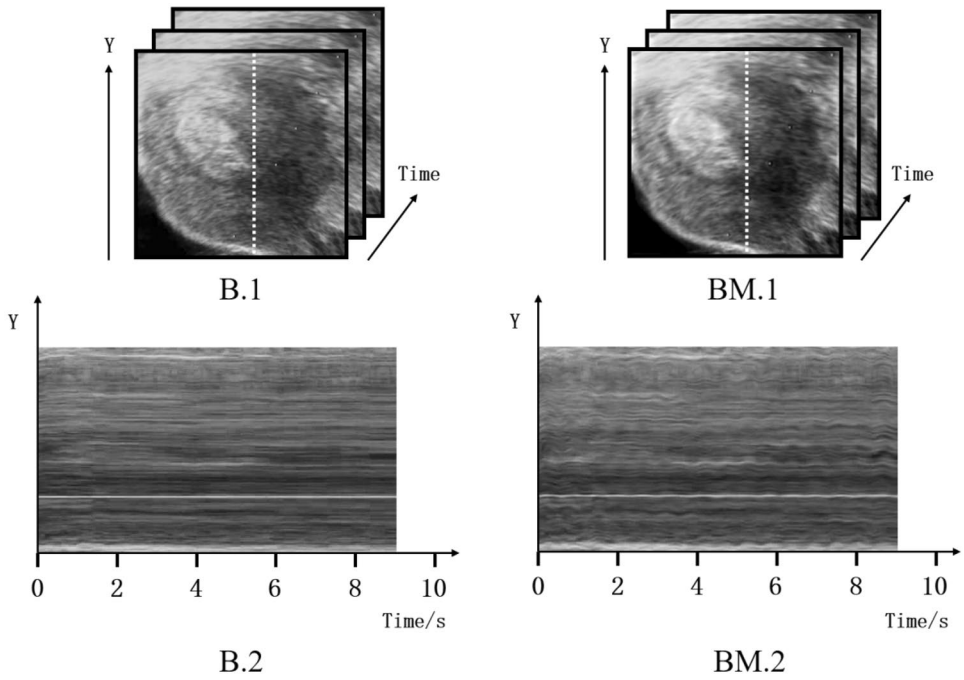

Fig. 4 Comparison of uterus video and magnified video from a typical pregnant patient (**B**) of IVF–ET. **B.1** represents the uterus video; **BM.1** represents the corresponding magnified video. **B.2** is the spatiotemporal YT slice of the uterine video, which is generated by the white dotted line's *Y* axis in uterus video. **BM.2** is the spatiotemporal YT slice of magnified video, which is generated by the white dotted line's *Y* axis in the magnified video

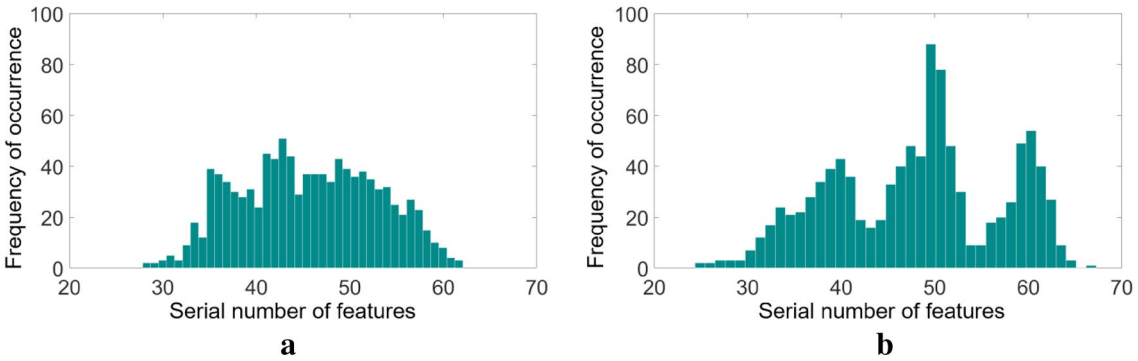

Fig. 5 Comparison of two typical DCD results based on magnified video between **a** typical non-pregnant patient and **b** typical pregnant patient. The horizontal axis is the number of different spatiotemporal patterns, and the vertical axis is the corresponding frequency of occurrence

The logistic regression analysis identified the HEMEW as an independent determinant of IVF–ET outcome (Table 2) among other factors in Table 1. The odds ratio (OR) of HEMEW was greater than one, which indicated that the HEMEW presented a positive association with pregnancy outcome in IVF–ET.

ROC analysis was used for HEMEW. The threshold (cutoff value) of HEMEW was 70.01 (AUC = 0.774; 95% CI = 0.644–0.905), whose accuracy was 72.6%, sensitivity was 75.9%, and specificity was 77.3% (as shown in Fig. 7).

Discussion

First, encouraged by clinical experiences and the phase-based motion magnification techniques [16], we identified the existence of uterine micro-peristalsis by introducing video magnification. Second, we demonstrated that the UMP could help to effectively distinguish clinical pregnancy outcomes of IVF–ET by dynamic feature extraction.

There were four reasons to support the existence of the hypothesized UMP: (1) the qualitative results were the visualization of invisible UMP; (2) the quantitative results illustrated that the HEMEW exhibited a satisfactory performance in distinguishing outcomes of IVF–ET; (3) the meaning of HEMEW was consistent with previous

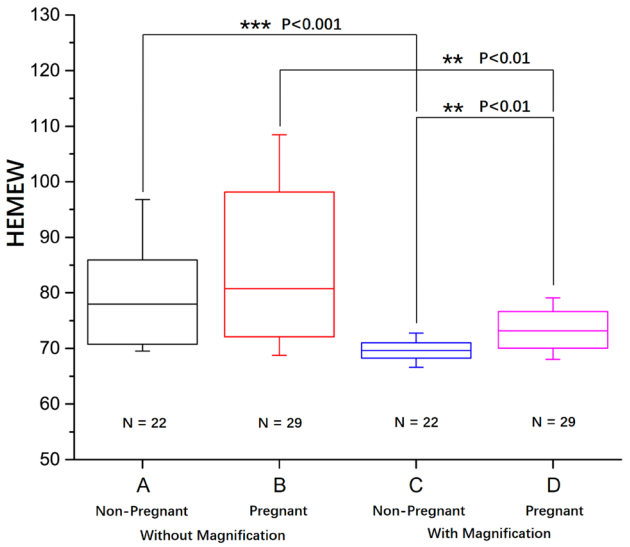

Fig. 6 Comparison of HEMEW in non-pregnant and pregnant patients in IVF–ET. **A** is the non-pregnant patients without video magnification, **B** is the pregnant patients without magnification, **C** is the non-pregnant patients with magnification, **D** is the pregnant patients with magnification. The HEMEW with magnification of **C** and **D** has significant difference ($p = 0.0033 < 0.01$, $n = 51$), while the HEMEW without magnification of **A** and **B** has no significant difference. **A**, **C** has significant difference ($p = 0.0008 < 0.001$, $n = 51$). **B** and **D** has significant difference ($p = 0.0026 < 0.01$, $n = 51$)

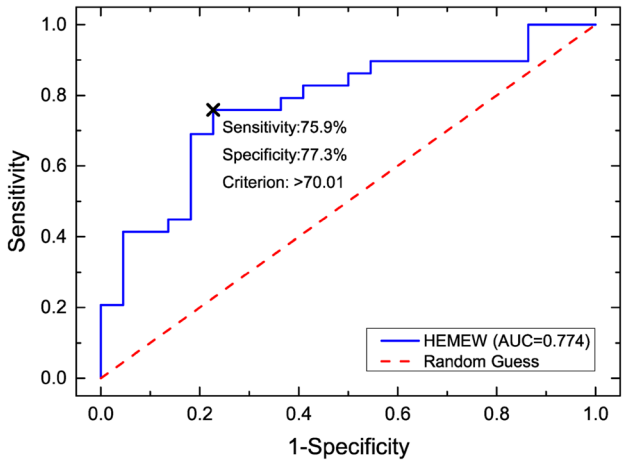

Fig. 7 The ROC curve of HEMEW. The cutoff value of HEMEW is 70.01. × is the cutoff point with corresponding sensitivity and specificity

studies; (4) we have conducted enough measures to eliminate the influence of other factors; the logistic regression analysis and ROC analysis supported this conclusion.

Consistency with previous studies

Previous studies proved that the uterus was inherently peristaltic, and its peristalses played an important role in sperm transport [13], embryo movement [14] and implantation [15]. Some even claimed that these peristalses were also related to clinical pregnancy outcome in fresh and frozen-thawed embryo transfer cycles [15]. Thus, it is reasonable to believe that UMP may be strongly related to the outcome of IVF–ET.

Besides, our results with video magnification were consistent with previous studies which revealed that abnormal uterine peristalsis was linked to decreased pregnancy rate [15, 20, 21]. The proposed index HEMEW describes the complexity of uterine micro-peristalsis. The higher the value of HEMEW, the more complex the uterine micro-peristalsis. The more complex the uterine micro-peristalsis the lower the uterine peristalsis, which is explained by physiological interpretation below. The result in Fig. 6 demonstrates that pregnant patients have higher HEMEW than non-pregnant patients. That is to say, the UMP of non-pregnant patients is abnormal, compared to that of pregnant patients, which is consistent with previous researches.

Physiological interpretation

There is a proposed physiological interpretation for UMP. Given that uterine peristalsis was occasionally visible by naked eyes clinically, we speculated that the uterus peristalsis might be the synchronization of many uterine micro-peristalses, which we named as UMP. This phenomenon is similar to the emergence phenomena in an ant colony [22]. The more complex the direction of each component force, the smaller the resultant force.

Given previous findings [10–12] that local blood supply is related to outcome of IVF–ET, we further speculated that the incidence of UMP might be positively correlated to the local blood supply either. The magnify frequency range of 1–1.7Hz and planes = 19 were chosen to match the human heart rate, which mainly reflects the influence of blood flow. This provides evidence for the assumption that UMP may be related to blood flow.

Efforts to reduce the impact of other factors on UMP

Since there are so many confounders that could influence the detection of UMP, we taken necessary measures to reduce the effects of these independent factors.

All the patients enrolled in our study were well controlled with many clinical factors that could influence IVF–ET's

outcome, such as age, BMI, bFSH, and so on, which were showed in Fig. 1.

To reduce the effect of different size of the uterus and endometrium, we applied normalization to the image size of uterus. Every picture of uterus was resized to the resolution of 256 × 256. The uterus which is larger than 256 × 256 would be scaled down to 256 × 256, and the uterus which is smaller than 256 × 256 would be scaled up to 256 × 256. So, the effects of varying thicknesses of endo- and myometrium were highly reduced.

To decrease the influence of different uterine positions, we applied VLPQ algorithm to obtain the features of UMP. The VLPQ has rotation invariance. That is to say, the rigid rotation changes of the uterus do not affect the features of UMP extracted by VLPQ algorithm. Inspired by the successful application of volume local binary patterns in facial expression recognition [23], the extended VLPQ algorithm, which is based on frequency domain features and adept at rotational invariance, was utilized to extract the dynamic characteristics of uterine micro-peristalsis. Thus, the VLPQ algorithm does not need to forcefully standardize the orientation of the entire uterus in the preprocessing stage. We also noticed that UMP and facial expression are quite similar in two aspects: one is that uteruses in ultrasound videos are egg shaped, the similar shape of human faces; and another is that facial expressions shift facial organs, just like peristalses in the uterus.

To cut down the impact of shaking hand, which holds the transvaginal probe, we designed and fabricated a probe fixer. The previous study revealed that traditional TVUS could not objectively measure contraction amplitude [17], because the clinicians held the TVUS probe to scan the uterus and their shaking hand might lead to shaking images, either visible or invisible, which resulted in the subjective scanning result. Our probe fixer can tackle this problem, as shown in Fig. 2. It replaces the clinicians' hand in a stable state with no shaking.

Probe orientation and video quality are highly operator dependent [17]. To overcome this difficulty, we have set up a standardized scanning protocol which is shown in Materials and Methods. In this study, only one operator (clinician) performed scanning.

Patients' breaths would have slight effect on the detection of UMP, so we designed the algorithm to drastically reduce their impact. The frequency band of video magnification was set as 1–1.7 Hz, which did not cover the breath rate (0.2–0.33 Hz). That is to say, the breath effect to the uterus was not magnified by video magnification algorithm.

To reduce the phase noise due to possible motion artifacts of uterus neighbor tissues, we manually selected the uterus ROIs for further magnification. Compared with the classical Euler video magnification [24], the phase-based video magnification only transferred the noise without amplifying them [16], which is more suitable for ultrasound video with a relatively lower signal-to-noise ratio in this study.

For the sake of controlling the factors that may affect the uterine micro-peristalsis and pregnancy outcome, we screened the patients enrolled in this study. These patients were 32.75 ± 3.52 years old, and the average number of oocytes retrieved was 10.44 ± 6.63. Among them, the proportion of poor pregnancy outcome was low, such as poor ovarian response (POR) of patients which was only 9.8%. All these indicated that most of the patients had a good ovarian reserve, and then gained a slightly high clinical pregnancy rate (56.86%).

Though there was a significant difference in fasting glucose ($p < 0.05$), the mean fasting glucose was normal, which revealed no clinical value in this study. So this significant difference was a data bias due to the small sample. As we know, insulin resistance is more valuable than fasting glucose, but there was no significant difference in insulin resistance. Moreover, the insulin resistance had no significant influence on pregnancy outcome according to the logistic regression analysis. All these meant that the significant difference in fasting glucose had no significant effect on the outcome of IVF–ET in the present study.

Strengths and limitations

Our study exhibits three strengths: first, UMP could be observed all the time by proposed method, which successfully solves the problem that uterine peristalsis cannot be seen at any moment and do not occur in the uterus because of some diseases; second, the data collection method of UMP is low cost, time saving, and noninvasive [25]. Third and foremost, UMP is believed to be a new independent factor related to the pregnancy outcome of IVF–ET. Moreover, it can be observed in all kinds of the uterus as it is assumed to be driven by blood flow, and may have different characteristics associated with diseases. Drugs such as oxytocin might regulate the peristalsis of the uterus clinically [26] and improve clinical pregnancy outcome. Therefore, UMP may also have potential clinical value in prediction and the intervention for IVF–ET.

Nevertheless, our study holds two limitations: the operator has to obey the standardized data collection protocol via probe fixer; patients have to remain still while being scanning. A three-dimensional ultrasound probe with a sophisticated image registration algorithm could be done to overcome these limitations.

Conclusion

In conclusion, it is reasonable to believe the existence of uterine micro-peristalses by visualization, quantitative index HEMEW, and control of other factors. Our method might

provide a valuable tool to distinguish pregnancy outcome of IVF–ET and help in better understanding endometrial receptivity.

Acknowledgements The authors acknowledge Beijing Municipal Science & Technology Commission for providing grants (No. Z181100001718132) from the Capital Clinical Medical Application and Development Funds.

Author contribution YFL: project development, data management, data analysis, manuscript writing and editing, literature research. RL: project development, data collection, data analysis, manuscript writing, literature research. JBZ: project development, data management, data analysis, manuscript writing, literature research. FF: project development, data collection, data management, literature research. CC: project development, data collection, data management. QL: project development, data collection, data management, data analysis, manuscript writing, literature research. JZ: project development, data management, data analysis, manuscript writing, literature research. All authors read and approved the final manuscript.

Compliance with ethical standards

Conflict of interest All authors declare that they have no conflict of interest.

Research involving human participants This study was approved by the Ethics Committee of Peking University People's Hospital (approval number: 2018PHB150-01). All procedures performed in studies involving human participants were in accordance with the ethical standards of the institutional research committee and with the 1964 Helsinki declaration and its later amendments or comparable ethical standards.

Informed consent Informed consent was obtained from all individual participants included in the study.

References

1. Kashir J et al (2010) Oocyte activation, phospholipase C zeta and human infertility. Hum Reprod Update 16(6):690–703
2. Guh R-S, Wu T-CJ, Weng S-P (2011) Integrating genetic algorithm and decision tree learning for assistance in predicting in vitro fertilization outcomes. Expert Syst Appl 38(4):4437–4449
3. Daido S et al (2013) Anticholinergic agents result in weaker and shorter suppression of uterine contractility compared with intestinal motion: time course observation with cine MRI. J Magn Reson Imaging 38(5):1196–1202
4. Leonhardt H et al (2012) Uterine morphology and peristalsis in women with polycystic ovary syndrome. Acta Radiol 53(10):1195–1201
5. Van Gestel I et al (2003) Endometrial wave-like activity in the non-pregnant uterus. Hum Reprod Update 9(2):131–138
6. Ledee-Bataille N et al (2002) Concentration of leukaemia inhibitory factor (LIF) in uterine flushing fluid is highly predictive of embryo implantation. Hum Reprod 17(1):213–218
7. Gonen Y et al (1989) Endometrial thickness and growth during ovarian stimulation: a possible predictor of implantation in in vitro fertilization. Fertil Steril 52(3):446–450
8. Noyes N et al (1995) Implantation: endometrial thickness appears to be a significant factor in embryo implantation in in-vitro fertilization. Hum Reprod 10(4):919–922
9. Gonen Y, Casper RF (1990) Prediction of implantation by the sonographic appearance of the endometrium during controlled ovarian stimulation for in vitro fertilization (IVF). J In Vitro Fertil Embryo Transf 7(3):146–152
10. Chien L-W et al (2002) Assessment of uterine receptivity by the endometrial-subendometrial blood flow distribution pattern in women undergoing in vitro fertilization-embryo transfer. Fertil Steril 78(2):245–251
11. Wang L et al (2010) Role of endometrial blood flow assessment with color Doppler energy in predicting pregnancy outcome of IVF-ET cycles. Reprod Biol Endocrinol 8(1):122
12. Sardana D et al (2014) Correlation of subendometrial-endometrial blood flow assessment by two-dimensional power Doppler with pregnancy outcome in frozen-thawed embryo transfer cycles. J Hum Reprod Sci 7(2):130
13. Kunz G, Leyendecker G (2002) Uterine peristaltic activity during the menstrual cycle: characterization, regulation, function and dysfunction. Reprod Biomed Online 4:5–9
14. Orisaka M et al (2007) A comparison of uterine peristalsis in women with normal uteri and uterine leiomyoma by cine magnetic resonance imaging. Eur J Obstet Gynecol Reprod Biol 135(1):111–115
15. Zhu L et al (2014) Uterine peristalsis before embryo transfer affects the chance of clinical pregnancy in fresh and frozen-thawed embryo transfer cycles. Hum Reprod 29(6):1238–1243
16. Wadhwa N et al (2013) Phase-based video motion processing. ACM Trans Gr (TOG) 32(4):80
17. Kuijsters NPM et al (2017) Uterine peristalsis and fertility: current knowledge and future perspectives: a review and meta-analysis. Reprod Bio Med 35(1):50–71
18. Ojansivu V, Heikkilä J (2008) Blur insensitive texture classification using local phase quantization. In: International conference on image and signal processing. Springer
19. Tzeng G-H, Huang J-J (2011) Multiple attribute decision making: methods and applications. Chapman and Hall/CRC, Cambridge
20. Yoshino O et al (2010) Decreased pregnancy rate is linked to abnormal uterine peristalsis caused by intramural fibroids. Hum Reprod 25(10):2475–2479
21. Yoshino O et al (2012) Myomectomy decreases abnormal uterine peristalsis and increases pregnancy rate. J Minim Invasive Gynecol 19(1):63–67
22. Johnson S (2002) Emergence: the connected lives of ants, brains, cities, and software. Simon and Schuster, New York
23. Dhall A et al (2011) Emotion recognition using PHOG and LPQ features. In: 2011 IEEE international conference on automatic face & gesture recognition and workshops (FG 2011). 2011. IEEE
24. Wu H-Y et al (2012) Eulerian video magnification for revealing subtle changes in the world
25. Celiesiute J et al (2017) Transvaginal ultrasound-noninvasive method for the prediction of response to concurrent chemoradiotherapy in cases of cervical cancer. J Vibroeng 19(3):2180–2187
26. Kunz G et al (1998) Uterine peristalsis during the follicular phase of the menstrual cycle: effects of oestrogen, antioestrogen and oxytocin. Hum Reprod Update 4(5):647–654